

Molecular composition of dissolved organic matter in the Mediterranean Sea

Alba María Martínez-Pérez ^{1,*} Helena Osterholz ² Mar Nieto-Cid,¹ Marta Álvarez,³ Thorsten Dittmar,² Xosé Antón Álvarez-Salgado¹

¹Consejo Superior de Investigaciones Científicas – Instituto de Investigaciones Mariñas (CSIC-IIM), Vigo, Spain

²Research Group for Marine Geochemistry, Institute for Chemistry and Biology of the Marine Environment (ICBM), Carl von Ossietzky University, Oldenburg, Germany

³Instituto Español de Oceanografía (IEO), Centro Oceanográfico de A Coruña, A Coruña, Spain

Abstract

The molecular composition of marine dissolved organic matter (DOM) is still poorly understood, particularly in the Mediterranean Sea. In this work, DOM from the open Mediterranean Sea and the adjacent North-east Atlantic Ocean was isolated by solid-phase extraction (SPE-DOM) and molecularly characterized using Fourier-transform ion cyclotron resonance mass spectrometry. We assessed the gradual reworking of the SPE-DOM transported by the shallow overturning circulation of the Mediterranean Sea by following the increase in molecular weight (+20 Da), oxygenation (+5%), degradation index (Ideg +22%), and the proportional decrease of unsaturated aliphatic compounds (+34%) along the Levantine Intermediate Water. This reworked SPE-DOM that leaves the Mediterranean Sea through the Strait of Gibraltar strongly contrasts with the fresh material transported by the inflow of Atlantic water (Ideg –25%). In the deep eastern and western overturning cells, the molecular composition of the deep waters varied according to their area and/or time of formation. SPE-DOM of the waters formed in the Aegean Sea during the Eastern Mediterranean Transient (EMT) was more processed than the DOM in pre-EMT waters formed in the Adriatic Sea (molecular weight and the proportion of unsaturated aliphatic compounds were increased by 5 Da and 9%, respectively). Furthermore, pre-EMT waters contain more reworked SPE-DOM (Ideg +7%) than post-EMT waters formed also in the Adriatic Sea. In summary, our study shows that the Mediterranean Sea constitutes a laboratory basin where degradation processes and diagenetic transformations of DOM can be observed on close spatial and temporal scales.

Marine dissolved organic matter (DOM) is one of the largest and least understood reservoirs of reduced carbon on the Earth's surface (Hedges 1992; Hansell 2002). At 662 Pg C, DOM represents 96% of the total organic carbon in the oceans (Hansell et al. 2009). It is produced mainly in the epipelagic layer (0–150 m depth) as a result of phytoplankton photosynthesis and subsequent food web interactions (Carlson 2002). Most of this recently produced DOM is quickly respired to CO₂. However, a small fraction of this material escapes rapid mineralization, accumulating in the upper layers for eventual export to the dark ocean (> 150 m depth) by convective overturning and vertical mixing (Hansell et al. 2009).

To achieve a better understanding of the fate of DOM in the dark ocean, identifying the molecular composition and structure of this material is essential. Previous studies applying ¹H nuclear magnetic resonance (NMR), amino acid, and neutral sugar analysis of ultrafiltered DOM (UDOM) revealed that carbohydrates are main constituents of this material at the sea surface of the Mediterranean Sea (Jones et al. 2013). This pool decreases with depth indicating DOM biodegradation. In addition, a strong correlation between amino acid concentration, apparent oxygen utilization (AOU), and picoplankton activity has been observed (Meador et al. 2010; Jones et al. 2013).

Tangential-flow ultrafiltration with a 0.5–1 kDa cut-off is able to isolate up to 30% of marine DOM (Benner et al. 1992; Amon and Benner 1996; Benner et al. 1997). Solid-phase extraction (SPE) using styrene divinyl benzene polymer (PPL) cartridges has more recently been introduced as an efficient method for isolating more than 60% of marine

*Correspondence: albam@iim.csic.es

Additional Supporting Information may be found in the online version of this article.

DOM (Dittmar et al. 2008; Green et al. 2014). The salt-free extracts are accessible by modern, nontargeted ultrahigh-resolution analytical techniques such as Fourier-transform ion cyclotron resonance mass spectrometry (FT-ICR-MS) for a comprehensive characterization. Nowadays, FT-ICR-MS is a widely used technique to distinguish thousands of molecular formulae constituting the DOM pool. Previous studies on the molecular composition of DOM by FT-ICR-MS showed molecular level differences between terrestrial and marine DOM (Koch et al. 2005), open ocean and coastal DOM (Koprivnjak et al. 2009) as well as surface and deep water DOM in the North Pacific (Medeiros et al. 2015) and North Atlantic (Hansman et al. 2015) oceans. Furthermore, the effect of degradation on the molecular composition of DOM was investigated along the eastern Atlantic and Southern Oceans combining FT-ICR-MS with radiocarbon analysis (Flerus et al. 2012; Lechtenfeld et al. 2014). Hertkorn et al. (2006) combined multidimensional NMR with FT-ICR-MS on UDOM, reporting carboxylic-rich alicyclic molecules (CRAM) as a likely major component of the DOM (8% of the whole DOM pool). More studies exist on the molecular characterization of open ocean DOM by FT-ICR-MS (Hertkorn et al. 2006; Chen et al. 2014; Hansman et al. 2015; Medeiros et al. 2015), but DOM composition in the enclosed Mediterranean Sea has not been studied in this detail yet.

The Mediterranean Sea is considered a concentration basin (evaporation > precipitation + runoff) characterized by low nutrient concentrations. This is due to the imbalance between the bottom outflow of nutrient-rich Mediterranean Water and the surface inflow of nutrient-poor Atlantic water (AW) at the Strait of Gibraltar (Huertas et al. 2012). High oxygen concentrations in the deep layers are a consequence of the recent formation of the Mediterranean deep waters (Cruzado 1985). Relatively small in size, the Mediterranean Sea has been used as a test basin for general ocean circulation studies (Béthoux et al. 1998; Bergamasco and Malanotte-Rizzoli 2010). The time scale of the Mediterranean Sea meridional overturning circulation is about 50–80 yr (Pinardi and Masetti 2000), compared to about 350 yr for the world ocean (Laruelle et al. 2009).

During the HOTMIX cruise (April–May 2014), we collected samples at selected depths along a longitudinal transect from the Levantine Sea to the Northeast Atlantic Ocean to characterize the molecular composition of solid-phase extractable DOM (SPE-DOM) through the water column via FT-ICR-MS. The specific objectives of our study are to (1) determine the overall molecular composition of the SPE-DOM in the Mediterranean Sea; (2) compare the molecular composition between the inflow of Atlantic surface water entering the Mediterranean Sea and the overflow of Mediterranean water into the Atlantic Ocean; and (3) explore the main drivers controlling the DOM transformations through changes in the molecular characteristics of SPE-DOM in

relation to the “oceanographic model system” of the Mediterranean Sea.

Materials and methods

Study site

The Mediterranean Sea is a semi-enclosed basin opened to the Atlantic Ocean through the Strait of Gibraltar. It is constituted by two basins of similar size, western and eastern, connected via the Strait of Sicily. The main water masses observed in the Mediterranean Sea are the AW in the epipelagic layer, the Levantine Intermediate Water (LIW) in the mesopelagic layer, and the Eastern (EMDW) and Western (WMDW) Mediterranean Deep waters in the bathypelagic layer. The Atlantic inflow enters the Strait of Gibraltar as a surface current of salinity (S) about 36.5, being slightly modified through evaporation and mixing with the outflowing Mediterranean waters, leading to the modified Atlantic water, which moves toward the East through a shallow and open thermohaline cell that spans the two basins and leads to the formation of intermediate waters in the eastern basin (Tsimplis et al. 2006; Bergamasco and Malanotte-Rizzoli 2010). These intermediate waters are formed by convection in the south of Rhodes (LIW) and in the Aegean Sea (Cretan intermediate water) and are found along the whole Mediterranean Sea between 200–500 m depth (Roether et al. 1998; Tsimplis et al. 2006). They present the maximum salinity of the Mediterranean water masses and outflow at the Strait of Gibraltar (Emelianov et al. 2006). The EMDW is formed in the Ionian Sea when water from the Southern Adriatic Sea plunges down through the Strait of Otranto and sinks to depths > 3000 m. Then, it flows eastward and occupies the water column below the LIW in the eastern Mediterranean basin presenting potential temperatures > 13.3°C and salinities > 38.66 (Wu et al. 2000). For a short period of time, during the Eastern Mediterranean Transient (EMT) in the middle 1990s, the main deep-water formation area was the Aegean Sea due to an abrupt shift in the climate and hydrography in this area, providing a warmer, more saline and denser deep water mass than the previously existing EMDW of Adriatic origin (Roether et al. 1996; Lascaratos et al. 1999; Klein et al. 2003). Hence, pre- and post-EMT varieties of EMDW of Adriatic origin coexists in the bathypelagic layer of the eastern basin. On the other basin, the WMDW is formed in winter in the Gulf of Lions (Gascard 1978) and occupies the water column below the LIW in the western Mediterranean basin with temperatures between 12.75°C and 12.80°C and salinities between 38.44 and 38.46 (Millot 1999). During the winter of 2004–2005, a strong convection event in the Gulf of Lions (Western Mediterranean Transition) led to the formation of a new WMDW variety, saltier and slightly warmer than previously (salinity of 38.47–38.50 and temperature of 12.87–12.90°C compared to 38.41–38.47 and 12.75–12.92°C; López-Jurado et al. 2005; Beuvier et al.

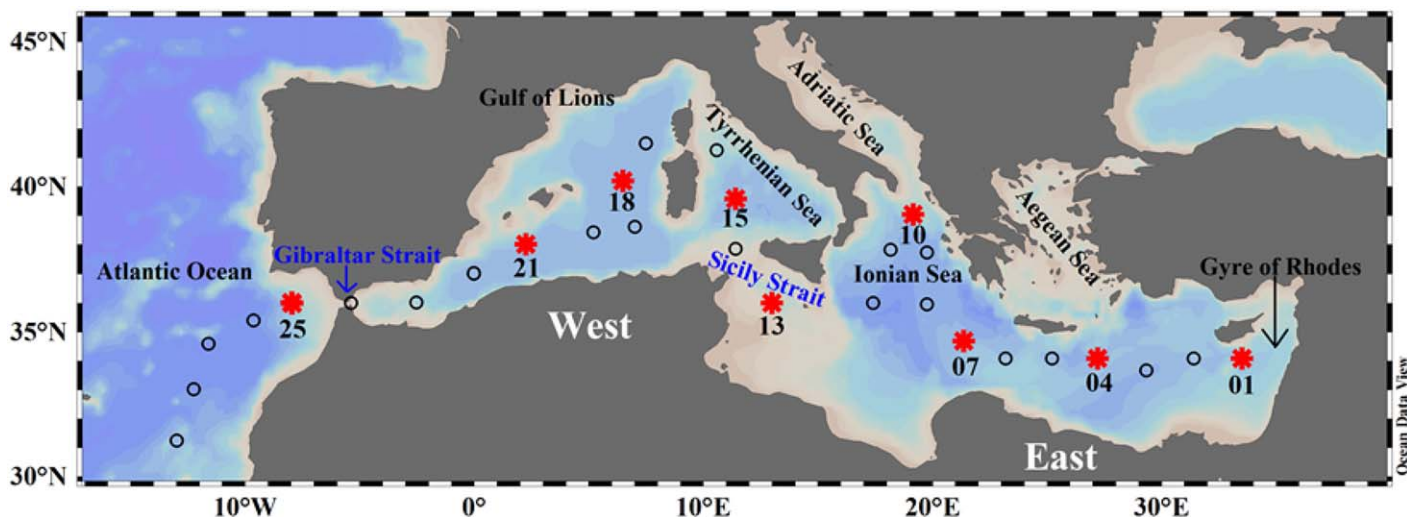


Fig. 1. Study area and sampling stations. The circles depict all cruise stations and asterisks represent the stations where samples were taken for molecular characterization of the DOM. Figure created using ODV software (Schlitzer 2016).

2012; Schroeder et al. 2016). Therefore, in the bathypelagic layer of the western Mediterranean, different varieties of WMDW coexist as well.

Sampling and determination of core parameters

Water samples were collected during the trans-Mediterranean cruise HOTMIX aboard R/V *Sarmiento de Gamboa* in spring 2014 (Heraklion, Crete, 27 April—Las Palmas, Canary Islands, 29 May). The transect consisted of 24 stations crossing the Mediterranean Sea from the Levantine Basin to the Strait of Gibraltar and 5 stations in the adjacent Northeast Atlantic Ocean (Fig. 1). At each station, full-depth continuous conductivity-temperature-depth (SBE 911 plus CTD probe), dissolved oxygen (DO; SBE-43 oxygen sensor) and chlorophyll fluorescence (SeaPoint fluorometer) profiles were recorded. Water samples were collected to analyze salinity, DO, and chlorophyll *a* (Chl *a*) to calibrate the sensors for conductivity, DO, and fluorescence, respectively. Conductivity measurements were converted into practical salinity scale values (UNESCO 1985). Samples for salinity were measured with a Guildline Portasal salinometer Model 8410A. Chl *a* concentration was determined in seawater samples (500 mL) filtered through Whatman GF/F filters and stored frozen until analysis. Pigments were extracted in cold acetone (90% v/v) for 24 h and analyzed by means of a 10 AU Turner Designs bench fluorometer, previously calibrated with pure Chl *a* (Sigma Aldrich), according to Holm-Hansen et al. (1965). DO was determined following the Winkler potentiometric method modified after Langdon (2010). The AOU ($AOU = O_{2sat} - O_2$) was calculated using the algorithm proposed by Benson and Krause (UNESCO 1986) for oxygen saturation (O_{2sat}). Potential temperature (θ) was calculated using TEOS-10 (UNESCO 2010).

Collection of SPE-DOM samples

At nine stations (red asterisks in Fig. 1) water samples were collected for the solid phase extraction of DOM (SPE-DOM) to perform FT-ICR-MS analysis. Four to five depths were sampled depending on the bathymetry of the stations (Fig. 2), except for the site at the Strait of Sicily (Sta. 13) where only LIW was sampled due to its shallowness. The deep chlorophyll maximum (DCM) was sampled according to the maximum fluorescence intensity, the LIW was sampled at the absolute maximum of the salinity profile at each station, the oxygen minimum layer (OML) was established on basis of the absolute minimum of the DO profile, and the deep waters were sampled according to the salinity and temperature characteristic of the bathypelagic zone of the eastern and western Mediterranean basins (Fig. 2).

The sampling strategy was restricted by time constraints during the cruise, which limited the number of collected samples, especially in the bathypelagic layer where different varieties of deep waters were found. Unfortunately, we were not able to sample any station in the Ionian Sea, so we missed the youngest variety of the EMDW. Note that although the hydrographic properties of the OML sample at Sta. 4 are reported in Supporting Information Table S1, this sample was rejected from the FT-ICR-MS analysis due to a contamination problem.

Water samples were collected in 5-liter acid-cleaned polycarbonate carboys, and then stored in the dark at 13°C until filtration within 5 h. Filtration was performed through pre-combusted (450°C, 4 h) Whatman GF/F filters in an acid-clean all-glass filtration system under positive pressure with low flow of high purity N₂. Two-liters aliquots of the filtrate were collected in acid-cleaned polytetrafluoroethylene (PTFE) bottles for SPE-DOM. Approximately 10 mL of the filtrate

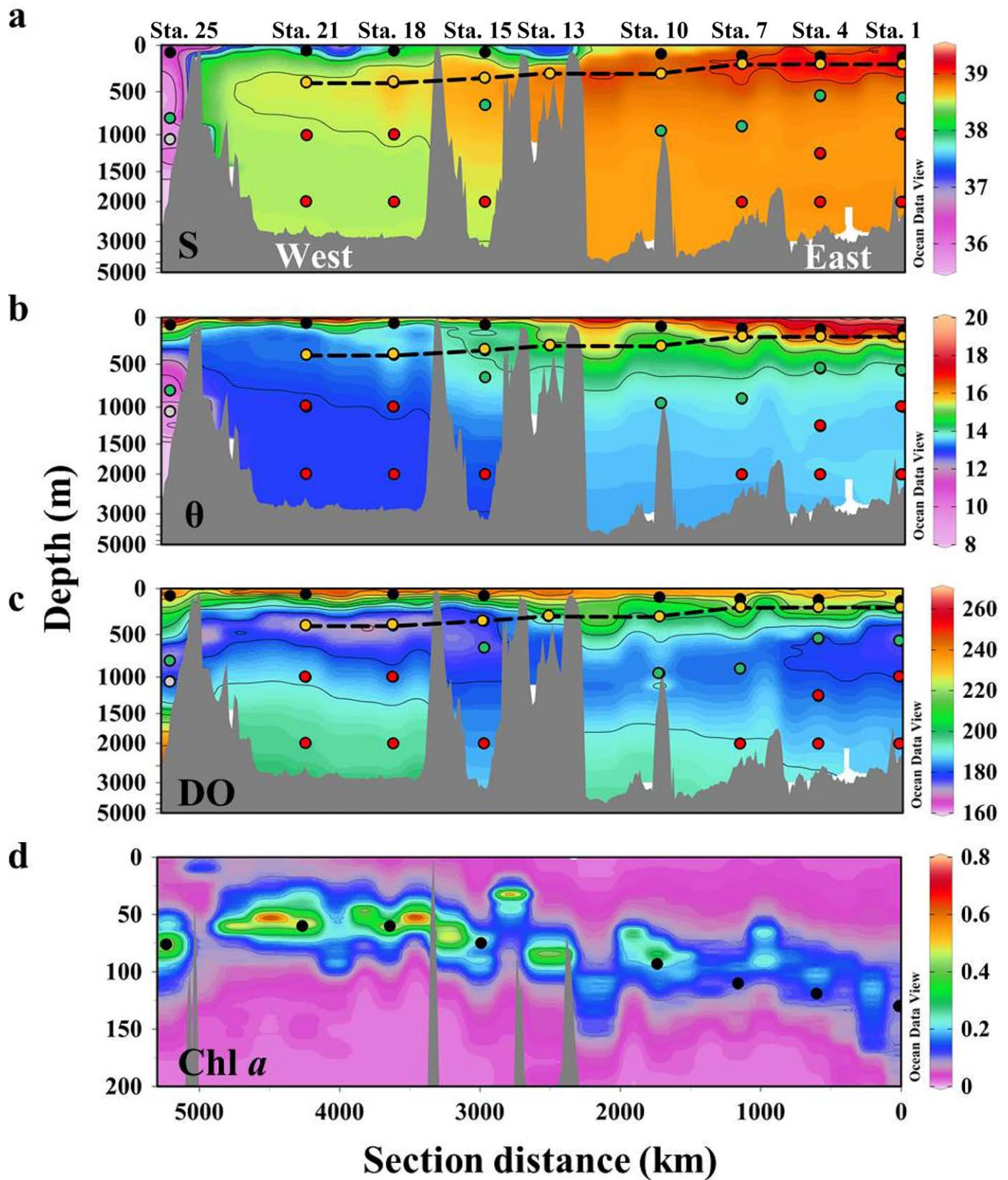


Fig. 2. Distribution of (a) salinity (S), (b) potential temperature (θ) in $^{\circ}\text{C}$, (c) DO in $\mu\text{mol kg}^{-1}$, and (d) fluorescence of Chl *a* in mg m^{-3} obtained from the sensors attached to the rosette sampler along the Mediterranean Sea. Black, yellow, green, and red dots represent samples taken in the epipelagic layer (DCM), LIW, OML, and deep waters, respectively. The dashed black line represents the route of the LIW along the transect. Note that the depth is displayed on a nonlinear scale. Values from all stations were used to show these distributions. Figure created using ODV software (Schlitzer 2016).

were collected for initial DOC determination in precombusted (450°C, 12 h) glass ampoules. These samples were acidified with H₃PO₄ (85%, p.a., Merck) to pH < 2, the ampoules were fire-sealed and stored in the dark at 4°C until analysis in the base laboratory. DOC concentrations were measured with a Shimadzu TOC-V organic carbon analyzer by high temperature catalytic oxidation. The system was calibrated daily with potassium hydrogen phthalate (99.95–100.05%, p.a., Merck). The precision of the equipment was ± 1 μmol L⁻¹. The accuracy was successfully tested daily with the DOC reference materials provided by D. A. Hansell (University of Miami, U.S.A.).

For SPE-DOM isolation, the filtered sea water sample (2 L) was acidified to pH 2 with HCl (37%, p.a., Merck) and the DOM was extracted on board with commercially available modified styrene divinyl benzene polymer cartridges (PPL, Agilent) as described in Dittmar et al. (2008). After extraction, cartridges were rinsed with acidified ultrapure water (pH 2, HCl 37%, p.a., Merck) to remove remaining salts and frozen at -20°C. Once in the base lab, the cartridges were dried by flushing with high purity N₂ and eluted with 6 mL of methanol (high pressure liquid chromatography (HPLC)-grade, Sigma-Aldrich). Extracts were stored in amber vials at -20°C. DOC concentrations in the extracts were measured after complete evaporation of an aliquot and re-dissolution in ultrapure water. The extraction efficiency is the ratio of SPE-DOC to initial DOC concentrations. The mean extraction efficiency was 47.3% ± 3.9% on a carbon basis. Some of the epipelagic water samples showed slightly lower extraction efficiencies, likely due to the fact that PPL cartridges do not efficiently elute/retain the larger molecules (Chen et al. 2016; Raeke et al. 2016), which can be a significant fraction of DOM in the surface mixed layer.

FT-ICR-MS analysis

SPE-DOM methanol extracts were diluted with ultrapure water and methanol (MS grade) to yield a DOC concentration of 15 mg C L⁻¹ and a methanol-to-water ratio of 1 : 1 (v/v). Duplicates of each sample were prepared for analysis by ultrahigh-resolution mass spectrometry using a Solarix FT-ICR-MS (Bruker Daltonik GmbH) connected to a 15 Tesla superconducting magnet (Bruker Biospin). Samples were infused at a flow rate of 120 μL h⁻¹ into the electrospray ionization source (ESI; Apollo II ion source, Bruker Daltonik GmbH) with the capillary voltage set to 4 kV in negative mode. Ions were accumulated in the hexapole for 0.3 s prior to transfer into the ICR cell. Data acquisition was done in broadband mode with a scanning range of 150–2000 Da. For each mass spectrum, 500 scans were accumulated. The spectra were mass calibrated (linear) using the Bruker Daltonics Data Analysis software package with an internal calibration list consisting of 51 known C_xH_yO_z molecular formulae over the mass range of the samples. With this calibration procedure, a mass error of <0.1 ppm was achieved. SPE-DOM

from the North Equatorial Pacific Intermediate Water (NEQ-PIW) collected at a depth of 670 m at the Natural Energy Laboratory of Hawaii Authority (NELHA) in Kona, Hawaii (Green et al. 2014) was used as an internal reference sample to assess instrument variability over time (Osterholz et al. 2014; Hansman et al. 2015). Molecular formulae were assigned to peaks considering a maximum mass error of 0.5 ppm and in the mass range between 150 Da and 850 Da by applying the following restrictions: ¹²C_{1–130}H_{1–200}O_{1–50}N_{0–4}S_{0–2}P_{0–2} as described in Seidel et al. (2014). Only compounds with a signal-to-noise (S/N) ratio of 4 and higher were used for further analysis. Moreover, compounds present in less than 20% of samples with a maximum S/N less than 20 were removed, as well as the molecules containing the following heteroatom combinations: NSP, N₂S, N₃S, N₄S, N₂P, N₃P, N₄P, NS₂, N₂S₂, N₃S₂, N₄S₂, and S₂P as these are less likely to occur in nature and, furthermore, to be more conservative in assigning molecular formulae to a given *m/z*. The FT-ICR-MS signal intensity of each identified molecular formula was normalized to the sum of all molecular formula intensities with S/N higher than 5 in each sample. We assumed that the inorganic (and organic) matrix is approximately the same for all the samples, so the intensity of each molecular mass is only affected by its concentration. Further, Seidel et al. (2015) incrementally mixed Amazon DOM with open Atlantic Ocean DOM showing that the response signal of ESI-FT-ICR-MS was linear to the mixing ratio. Therefore, we interpret the FT-ICR-MS data semi-quantitatively (Seidel et al. 2015; Hawkes et al. 2016). The analytical window of the FT-ICR-MS was restricted by both the SPE method and electrospray ionization efficiency. The SPE method, using PPL cartridges, allows to concentrate from the most apolar DOM species through to highly polar molecules, but not the smallest polar molecules (i.e., short chain organic acids and free amino acids) and colloidal aggregates (Chen et al. 2016; Hawkes et al. 2016; Raeke et al. 2016). ESI is a low-fragmentation technique that preferentially ionizes polar functional groups (Kujawinski 2002), therefore carbohydrates are likely less efficiently ionized by ESI than organic acids as it was suggested by Stubbins et al. (2010).

The aromaticity and the degree of unsaturation of a compound were assessed based on its molecular formula and were expressed as the modified aromaticity index (AI_{mod} = [1 + C - 1/2O - S - 1/2H - 1/2N - 1/2P]/[C - 1/2O - S - N - P]) and double bond equivalents (DBE = 1 + 1/2[2C - H + N + P]), respectively (Koch and Dittmar 2006, 2016). Higher AI and DBE are indicative of higher presence of aromatic or even condensed aromatic molecules (Koch and Dittmar 2006), which have been suggested to be resistant to biodegradation (Stubbins et al. 2010; Rossel et al. 2013). The degradation index (Ideg) was calculated using the formula proposed by Flerus et al. (2012) ranging between 0 and 1. It is used as a simple proxy to assess the relative degradation state of the SPE-DOM, and Flerus et al. (2012) suggested that a

higher Ideg points toward a more reworked DOM. The intensity-weighted averages of molecular weight, number of elemental atoms (C, H, O), number of heteroatoms (N, S, P), molar ratios (H/C, O/C, and C/N), AI_{mod} , and DBE were calculated for each sample by taking into account the FT-ICR-MS signal intensity of each assigned molecular formula. We sorted the assigned formulae into groups of formulae containing the following atoms: CHO, CHON, CHOS, CHOP, CHONS, and CHOSP. In addition, we assigned the identified molecular formula to compound groups based on established molar ratios, AI_{mod} , DBE and heteroatoms contents (Seidel et al. 2014). The compound groups used in this work were: (1) polyphenols ($0.5 < AI_{\text{mod}} < 0.666$) which are highly aromatic compounds, (2) highly unsaturated compounds ($AI_{\text{mod}} < 0.5$, $H/C < 1.5$, and $O/C < 0.9$), (3) unsaturated aliphatic ($1.5 < H/C < 2$, $O/C < 0.9$, and $N = 0$), and (4) carboxyl-rich alicyclic molecules (CRAM, $0.3 < DBE/C < 0.68$, $0.2 < DBE/H < 0.95$, and $0.77 < DBE/O < 1.75$) as described by Hertkorn et al. (2006). These parameters are summarized in Supporting Information Table S4. Note that 94% of the molecular formulae assigned to CRAM were also classified as highly unsaturated compounds. As this grouping includes a mixture of structural isomers and does not imply the presence of a structural entity in the sample (Seidel et al. 2014), we emphasize that this categorization is not unambiguous and alternative structures may exist for a given molecular formula. However, this classification is a useful tool to identify likely structures behind an identified molecular formula. All molecular parameters of each sample were calculated as averages of the duplicates.

Statistical analysis

Bray–Curtis dissimilarity matrices (Bray and Curtis 1957) were computed based on relative signal average intensities. Principal coordinates analysis (PCoA) was then used for graphical representation of the DOM variability on the first two major axes of compositional change. Environmental and calculated parameters were correlated to the PCoA factors and graphed accordingly (Pearson's product moment correlation). The analyses were performed in R (version 3.1.1, R Development Core Team 2012, [http://cran.r-project.org/]) and using the package vegan (Oksanen et al. 2016).

Multiple linear regressions were performed using R. Moreover, the Student's *t*-test was used for determining the significant differences between sample means (Supporting Information Table S3).

Results

Hydrography and bulk dissolved organic carbon background

Discrete sampling depths were chosen on basis of the vertical profiles of *S*, θ , DO, and Chl *a* (Fig. 2). The DCM (black dots in Fig. 2) was deeper in the eastern than in the western basin (Supporting Information Table S1), showing higher DO and Chl *a* in the western basin. Regarding the LIW, the

salinity maximum (yellow dots in Fig. 2) was found between 200 m and 300 m in the eastern basin, accompanied by a relative maximum of θ and DO. In the western basin, the salinity maximum was located deeper (between 350 m and 400 m) concurring with a relative maximum of θ and a minimum of DO. In general, the *S*, θ , and DO along the core of the LIW were lower in the western than in the eastern basin (Supporting Information Table S1; Fig. 2a–c). The OML (green dots in Fig. 2a–c) was found at 744 ± 211 m ($n = 4$) in the eastern basin. It coincided with the depth of the LIW in the western basin. Regarding the bathypelagic layer (red dots in Fig. 2), the eastern basin was dominated by the EMDW, which was saltier and warmer than the analogous waters in the western basin, dominated by the WMDW. DO values were similar in both basins.

DOC concentrations (Supporting Information Fig. S1 and Supporting Information Table S1) showed the maximum values of the sampling depths at the DCM ($> 60 \mu\text{mol L}^{-1}$), decreasing to a minimum of 43–44 $\mu\text{mol L}^{-1}$ in the deep waters. In the epipelagic layer, an inverse relationship between Chl *a* and DOC concentration was observed (Fig. 1d and Supporting Information Fig. S1a). It is remarkable that in the LIW the DOC decreased significantly from $60.2 \pm 0.9 \mu\text{mol L}^{-1}$ in the easternmost station (Sta. 1) to $47.4 \pm 0.7 \mu\text{mol L}^{-1}$ in the western basin (Sta. 18) (Supporting Information Fig. S1). Conversely, in the deep waters the distribution of the DOC did not reveal any significant gradient between the western and eastern basins. Our DOC concentrations confirmed the published vertical profile in both basins (Pujo-Pay et al. 2011; Santinelli 2015 and references therein). Atlantic samples showed similar DOC concentrations as the Mediterranean Sea samples (Supporting Information Fig. S1).

Mediterranean SPE-DOM molecular signatures

The distribution of the concentration of solid phase extracted DOC (SPE-DOC) was parallel to the concentration of the bulk DOC (Supporting Information Fig. S1) although carbon extraction efficiency was $47.3\% \pm 3.9\%$. SPE-DOC therefore constitutes a good proxy of the bulk DOC.

A total of 6057 resolved molecular masses of singly charged compounds were detected in the FT-ICR-MS spectra of the 32 SPE-DOM samples analyzed from the Mediterranean Sea and Northeast Atlantic Ocean, covering a mass range of 154–817 Da. We identified 3689 molecular formulae in the mass range of 157–736 Da, not considering ^{13}C isotopologues. The most abundant type of formulae was CHO, followed by CHON, CHOS, CHOP, CHONS, and finally CHOSP (Supporting Information Table S3).

The NEqPIW sample repeatedly analyzed as a reference sample to control the instrument variation over time also let us compare the molecular composition of the SPE-DOM in the Mediterranean Sea with one of the oldest water masses of the world ocean: NEqPIW (Supporting Information Table S3). As expected, we observe that the Mediterranean Sea

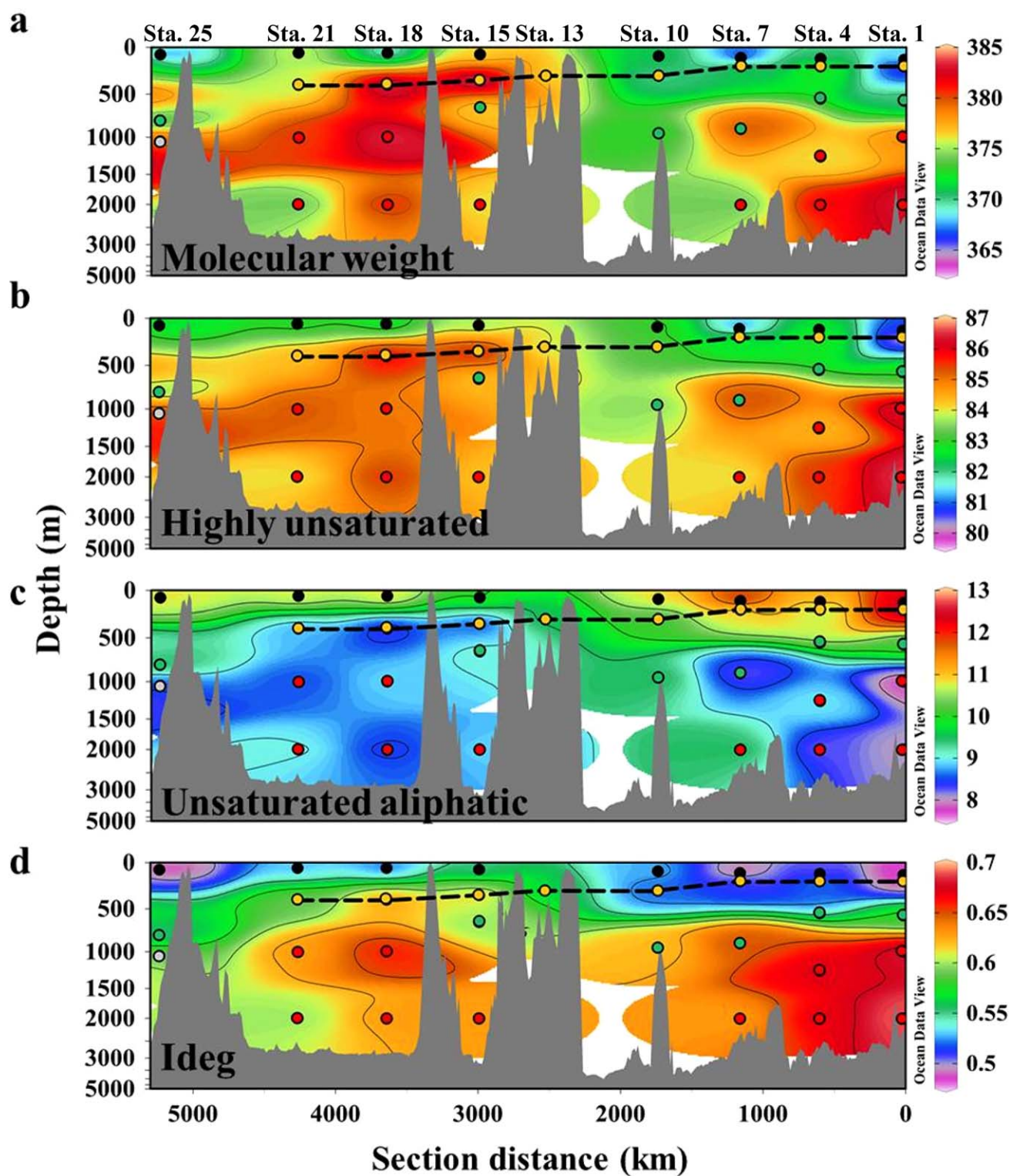


Fig. 3. Distributions of (a) molecular weight in Dalton, (b) highly unsaturated compounds in %, (c) unsaturated aliphatic compounds in %, and (d) Ideg (range between 0 and 1, unitless) using averages of duplicates in the Mediterranean Sea and Northeast Atlantic Ocean. The dashed black line represents the route of the LIW along the transect. Note that the depth is displayed on a nonlinear scale. Figure created using ODV software (Schlitzer 2016).

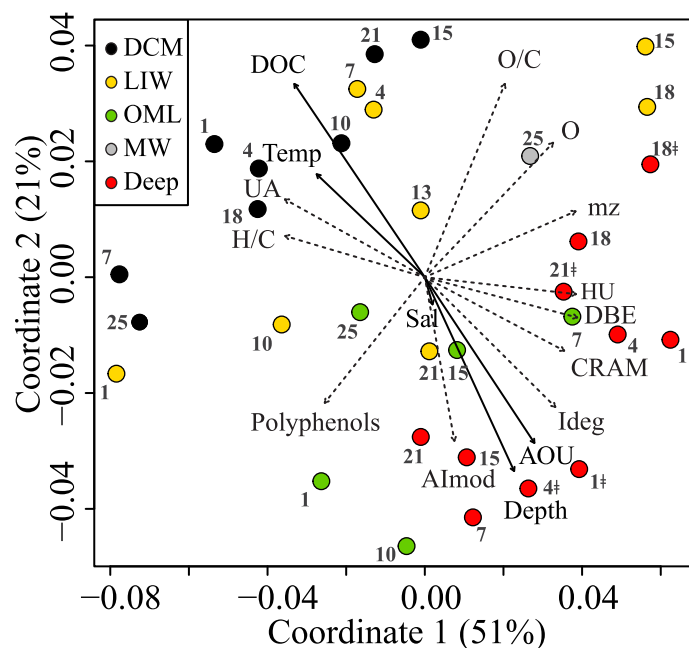


Fig. 4. PCoA of all detected molecular formulae and their normalized FT-ICR-MS signal intensities (averages of duplicates), based on Bray-Curtis dissimilarity of all samples, color coded by waters dominating in each layer. Environmental and calculated parameters fitted to the PCoA factors are shown with black bold and dashed arrows, respectively. HU, highly unsaturated compounds; Sal, Salinity; Temp, Temperature; UA, unsaturated aliphatic compounds. The symbol ‡ represents samples collected at 1000 m.

contains significantly less reworked DOM (lower molecular weight, O/C, DBE, and Ideg) than the NEqPIW.

The AW entering the Mediterranean Sea through the Strait of Gibraltar (represented by the DCM sample at Sta. 25; black dot in Fig. 3) exhibited a significantly different molecular composition than the overflow of Mediterranean water (represented by the LIW at Sta. 18; yellow dot in Fig. 3). Specifically, the SPE-DOM found in the AW inflow displayed lower molecular weight, O/C ratio, DBE, Ideg, CRAM, and highly unsaturated compounds contribution, as well as a higher proportion of unsaturated aliphatic compounds and an increased H/C ratio (Fig. 3 and Supporting Information Table S2). A PCoA to link molecular composition to environmental parameters that includes all samples (Fig. 4) also reveals the molecular dissimilarity between the Atlantic inflow and the Mediterranean overflow. While the Atlantic sample was found in the negative part of both axes, the LIW sample was found in the positive. Note that the first two coordinates of the PCoA comprised 72% of the SPE-DOM molecular variability. The differences between the inflow and outflow at the Strait of Gibraltar were also explored using a differential mass spectrum (Fig. 5a), subtracting the normalized peak intensities of the LIW at Sta. 18 from the normalized peak intensities of the DCM at Sta. 25. Positive differences of intensity showed peaks of higher relative

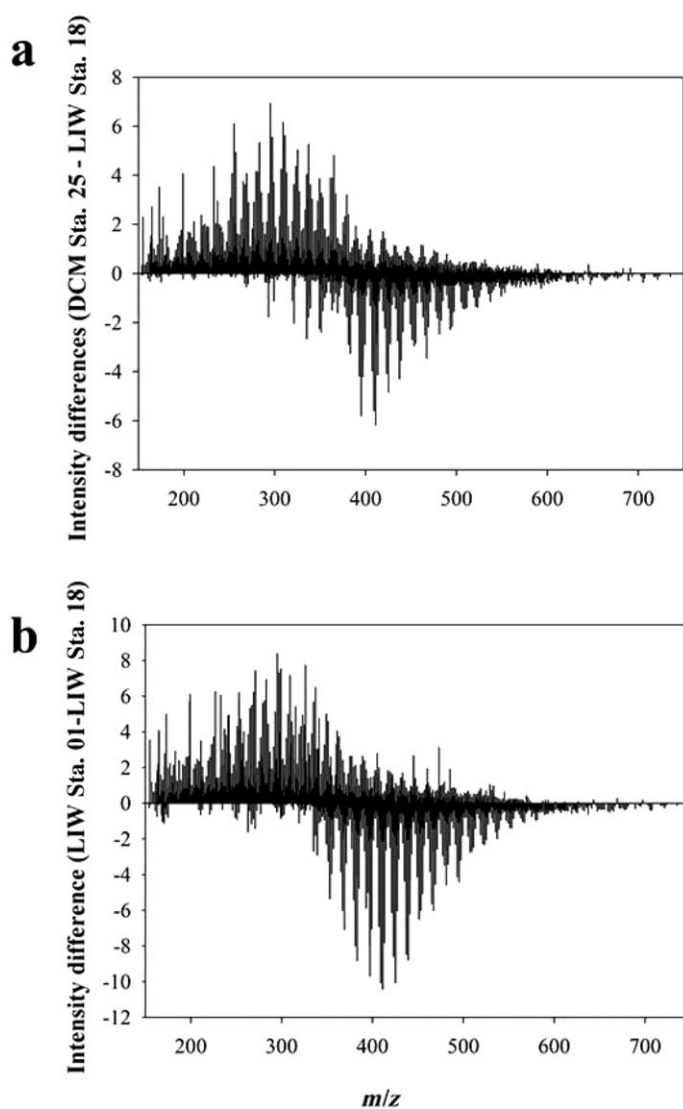


Fig. 5. Differences of FT-ICR-MS normalized signal intensities of SPE-DOM along a molecular mass scale (m/z) between (a) the inflow of AW collected at the DCM in Sta. 25 and the overflow of Mediterranean water represented by the LIW at Sta. 18, (b) LIW collected at Sta. 01 (near formation site) and LIW at Sta. 18 in the western basin. Positive differences correspond to higher relative intensities of DCM at Sta. 25 and LIW at Sta. 01 DOM, while negative differences correspond to higher relative intensities in the LIW Sta. 18 DOM, respectively, for (a) and (b) panels. The weighted average molecular mass of these differential spectra was calculated taking into account absolute peak heights of positive and negative peaks.

intensities in the Atlantic inflow with an average molecular weight of 349 Da. Negative signals indicated peaks of higher relative intensities in the Mediterranean overflow enriched in compounds of an average molecular weight of 432 Da. Note that LIW at Sta. 18 was chosen to represent the Mediterranean water overflow as LIW at Sta. 21 is influenced by the mixing with WMDW as it is located close to the deep waters in the θ/S diagram (Supporting Information Fig.

S2c) and apart from the LIW at Sta. 15 and 18 in the PCoA (Fig. 4).

To study the DOM degradation along the shallow overturning circulation cell of the Mediterranean Sea, we followed the compositional changes of SPE-DOM collected in the core-of-flow of the LIW. The molecular characteristics of the LIW samples were uneven and the samples were split in the PCoA (Fig. 4): while the eastern basin samples were found in the negative part of the first coordinate, the western basin samples were located in the positive. In addition, a constrained analysis of principal coordinates based on Bray-Curtis dissimilarities revealed significant molecular differences between both basins ($p < 0.05$, $n = 8$). Specifically, as the LIW flowed westward we observed a raise of molecular size (Fig. 3a), O/C ratio, DBE, and AI_{mod} . Moreover, we observed an increase of the Ideg and the proportion of highly unsaturated molecules, as well as a decrease of the proportion of unsaturated aliphatic molecules (Fig. 3b–d and Supporting Information Table S2). Again, these differences were examined in more detail using a differential spectrum (Fig. 5b), subtracting the normalized peak intensities of the LIW at Sta. 18 (western basin, more reworked DOM) from the normalized peak intensities of the LIW at Sta. 1 (eastern basin, fresher DOM). Positive differences of intensity showed peaks with higher relative intensities in the LIW at Sta. 1, where this sample presented an enrichment of molecules with an average molecular weight of 335 Da. Negative signals indicated peaks with higher relative intensities in the LIW at Sta. 18, sample enriched in molecules of an average molecular weight of 427 Da.

Concerning the deep waters, in the eastern basin, samples collected at 2000 m depth at Sta. 1 and 4 (EMT) fell closely together in the PCoA analysis (Fig. 4). However, the samples collected at 1000 m at Sta. 1 and 4 (pre-EMT) and at 2000 m at Sta. 7 (post-EMT) grouped in our ordination and were separated from the EMT samples. Comparing the molecular composition of SPE-DOM in these water masses, the deep water at Sta. 7 showed a less degraded SPE-DOM signature (lower molecular weight, oxygen, DBE, Ideg, highly unsaturated and higher contribution of unsaturated aliphatic compounds; Fig. 3 and Supporting Information Table S2).

Globally, the PCoA revealed a clear separation of the samples by water layers. Along both PCoA axes, less reworked DOM was clearly separated from more degraded DOM. Samples collected at the DCM (recently formed) were characterized by less reworked DOM (higher proportion of unsaturated aliphatic compounds, higher H/C ratio and DOC concentration). Highly unsaturated molecules, likely susceptible to photochemical processes, and photoresistant unsaturated aliphatic molecules comprised the largest fraction of the SPE-DOM (> 90%) in all samples (Supporting Information Table S2). Since abundances are expressed as relative contributions (percentages), the increase of one kind of compounds entails the decrease of the others. Thus, the lower

percentage of highly unsaturated compounds in the epipelagic layer (Fig. 3b) could be due to the photochemical removal of this type of molecules in the photic layer.

Discussion

Despite the relatively small size and short residence times of the Mediterranean Sea, a PCoA analysis revealed that the molecular composition of DOM was found to be heterogeneous among basins and water layers. We show that this heterogeneity is mainly caused by three different factors that control the DOM molecular composition in the Mediterranean Sea: water mass origin, biodegradation and photobleaching.

Water mass origin as a driver of SPE-DOM composition

We found that the overall molecular composition of the Mediterranean Sea was significantly less reworked than the NEqPIW (Supporting Information Table S3). This water mass acts a reference for refractory DOM, as it is one of the oldest, least ventilated, water masses of the global ocean (Stuiver et al. 1983; Osterholz et al. 2015). This result demonstrates the noticeable molecular differences between the Mediterranean Sea DOM and the NEqPIW DOM in spite of presenting similar radiocarbon ages as recently reported by Santinelli et al. (2015).

The exchange across the Strait of Gibraltar results in the Atlantic inflow transporting relatively fresh, nutrient-poor (Huertas et al. 2012), and less degraded DOC-rich surface AWs into the Mediterranean Sea. On the other hand, the Mediterranean outflow transports salty, nutrient-rich and reworked DOC-poor intermediate Mediterranean water into the Atlantic. Accordingly, Ideg and DBE of the SPE-DOC in the Mediterranean overflow increased by 25% and 5%, respectively, and the proportion of unsaturated aliphatic compounds decreased by 24% compared to the Atlantic inflow. Given that the AW that enters the Mediterranean Sea is part of the shallow overturning cell of the Mediterranean intermediate waters that constitute the Gibraltar overflow (Schneider et al. 2014), it is expected that the difference in composition is implemented during completion of that overturning circulation within the Mediterranean Sea basin. When the LIW is formed (Sta. 1), the DOM molecular composition is similar to the DOM Atlantic inflow (DCM in Sta. 25) (Sta. 25-black dot and Sta. 1-yellow dot in Fig. 4). However, once the LIW flows in the shallow overturning circulation across the Mediterranean Sea this water mass transports more degraded DOM as will be discussed in the next section.

Deep waters in the eastern basin exhibited significant molecular differences related to their formation site (Aegean vs. Adriatic) or time (pre- vs. post-EMT). Samples collected at 2000 m depth at Sta. 1 and 4 presented more degraded DOM (molecular weight increased by 5 Da, the proportion of polyphenols by 6% and the proportion of unsaturated aliphatic compounds decreased by 9%) than samples collected at 1000 m at the same stations (Figs. 3, 4; Supporting

Information Table S2). These molecular changes were attributed to the fact that samples collected at 2000 m were formed in the Aegean Sea during the EMT (according to their thermohaline properties and oxygen concentrations; Supporting Information Fig. S2d and Supporting Information Table S1; Roether et al. 1996, Lascaratos et al. 1999, Klein et al. 2003). However, samples collected at 1000 m were formed in the Adriatic Sea in the pre-EMT which showed lower S and DO concentration than the deep waters of Aegean origin (Lascaratos et al. 1999; Schneider et al. 2014). These results support the idea that water mass origin drives the DOM molecular composition. Regarding the formation time of these deep waters, it would be plausible that the oldest (pre-EMT) would host most degraded DOM, however, the results show the opposite. It seems that water mass origin has a higher impact on DOM molecular composition than water mass age in the deep waters of the eastern Mediterranean Sea. On the other hand, samples collected at 2000 m at Sta. 7 (post-EMT) presented less degraded DOM (lower molecular weight (-5 Da), Ideg (-7%), DBE (-2%), and an about 9% higher proportion of unsaturated aliphatic compounds) than the sample collected at Sta. 1 at 1000 m (pre-EMT). In this case, although both water masses were formed in the Adriatic Sea, their formation times were different according to their thermohaline properties and DO concentrations (Supporting Information Fig. S2d and Supporting Information Table S1), which lead to dissimilar DOM molecular signatures.

Diagenetic transformations of SPE-DOM through the Mediterranean Sea

The samples taken along the salinity maximum of the LIW show a total decrease in DOC concentration of $15 \mu\text{mol L}^{-1}$ attributed to prokaryotic degradation within the shallow overturning circulation of the Mediterranean Sea (black dashed line in Figs. 2a–c, 3). A highly significant linear relationship between DOC and AOU was found along the LIW pathway followed during the cruise ($r = -0.96$, $p < 0.001$, $n = 9$). The slope of this linear regression (model II; Sokal and Rohlf 1995) was -0.21 ± 0.02 , which, converted into oxygen equivalents using the canonical Redfield $-\text{O}_2/\text{C}$ ratio of 1.4, translates into 0.30 ± 0.03 , i.e., the $30\% \pm 3\%$ of the oxygen consumption was due to the microbial oxidation of DOC. To minimize the effect of water mass mixing on the DOC/AOU relationship, we performed a multiple linear regression of DOC with θ , S, and AOU. Doing this the slope changed to -0.31 ± 0.08 , which, converted into oxygen equivalents as above, resulted in a $43\% \pm 11\%$ of the oxygen consumption due to prokaryotic oxidation of DOC. Note that this number is not significantly different from the previously obtained with the simple linear regression. These values are consistent with previous estimates in the Mediterranean Sea by Santinelli et al. (2010, 2012), which ranged from 38% to 53%. Such a result is much higher than the 10–20% found

in the dark global ocean (Aristegui et al. 2002). Warmer deep-water temperatures in the Mediterranean Sea ($>13^\circ\text{C}$ vs. $<5^\circ\text{C}$; Dickson and Brown 1994), which stimulate the prokaryotic degradation processes, is the likely reason behind this difference. Microbial oxidation leads to decreasing DOC concentrations along the overturning cell and the remaining DOC is, indeed, more reworked. In this regard, in agreement with Hansman et al. (2015), we found a positive relationship between the Ideg and AOU for all collected samples: $\text{Ideg} = (0.0019 \pm 0.0002) \text{ AOU} + (0.50 \pm 0.01)$ ($R^2 = 0.71$, $p < 0.0001$). The obtained regression slope suggests that the degradation ratio per oxygen consumption unit is faster in the Mediterranean Sea than in the Atlantic Ocean, given that it is significantly higher ($p < 0.0001$) than the regression slope obtained by Hansman et al. (2015) in the Atlantic Ocean (slope = 0.00073 ± 0.00003 , $R^2 = 0.64$, $p < 0.001$). This more efficient degradation could also be related to the above mentioned warmer deep-water temperatures in the Mediterranean Sea. As a consequence, the rate of microbial processes would be about twofold higher in the Mediterranean Sea than in the Atlantic Ocean, according to the Arrhenius law. As for the case of DOC, to assess the role of water mass mixing in this relationship, we performed a multiple linear regression of Ideg with θ , S, and AOU ($R^2 = 0.80$; $p < 0.003$, Ideg/AOU slope = 0.0011 ± 0.0003). Whereas the standard deviation of Ideg ($\text{SD}_{\text{Ideg}} = 0.065$) retains the variability due to both water mass mixing and biogeochemical processes in the Mediterranean Sea, the standard deviation of the residuals of the multiple linear regression of Ideg with θ and S ($\text{SD}_{\Delta\text{Ideg}} = 0.035$) retains only the variability due to biogeochemical processes. Therefore, from the ratio of both SD, it can be inferred that 54% of the observed variability of Ideg could be explained by processes not associated to water mass mixing. We could presume that the mixing of LIW, with EMDW in the eastern basin and with WMDW in the western basin, can be partly responsible for the different molecular composition observed in the LIW of Sta. 1 and 18. However, in the western basin, mixing cannot be the only process affecting the LIW, since this water mass with the highest AOU is surrounded by water bodies (the DCM on top and the WMDW underneath) which present lower AOU values (Supporting Information Table S1). Concomitantly, part of the observed changes in the molecular composition of SPE-DOM could be due to the production/consumption of higher/lower molecular weight compounds as the LIW becomes older (more degraded) in its route westward. A parallel increase in molecular weight (Fig. 5b) and oxygenation (5%) and a decrease of the H/C ratio (Supporting Information Table S2) were found to be indicators of degraded organic matter (Flerus et al. 2012; Hertkorn et al. 2013, Chen et al. 2014), in accordance with an increase of the Ideg (22%). A higher DBE and AI_{mod} are indicative of an increasing degree of aromaticity and unsaturation (Koch and Dittmar 2006, 2016). In addition, a higher proportion of highly unsaturated compounds (7%) is also indicative of

reworked DOM, as these compounds are considered refractory and produced during the remineralization processes in the meso- and bathypelagic layers (Seidel et al. 2015). Conversely, unsaturated aliphatic compounds are considered bio-labile molecules, as they comprise a major fraction of phytoplankton exudates (Medeiros et al. 2015). We observed a decrease by 34% of the proportion of unsaturated aliphatic compounds in the LIW along its route westward.

Photodegradation vs. biodegradation in the epipelagic layer

Photochemical processes have been proposed as an abiotic pathway for DOC degradation in the surface ocean (Mopper et al. 2015). The Ideg is used to assess the degradation state of the SPE-DOM. Since photodegradation can produce bio-labile aliphatic and peptide-like compounds (Stubbins et al. 2010; Stubbins and Dittmar 2015), we hypothesize that this process could lead to a lower Ideg. We observed an increasing trend of Ideg with depth (Fig. 3d), likely indicating a synergy between an increasing contribution of prokaryote DOM degradation with depth, and the potential photodegradation and new production in the photic layer. However both processes, new production and photodegradation, cannot be deciphered by applying the Ideg. Therefore, we do not find conclusive evidence for the effect of photodegradation in the Mediterranean Sea, probably due to the great depth of the shallowest level that we sampled (DCM). In addition, the cruise was conducted in April–May, i.e., after winter mixing and when solar radiation is not at the summer maximum. Further studies/experiments should be performed to clarify the role of photochemical processing on the DOM composition in the Mediterranean Sea.

Conclusions

Despite the small size and relatively short residence time of the Mediterranean Sea, water mass origin and mineralization processes lead to contrasting molecular composition of SPE-DOM with depth and basin. SPE-DOM in the Mediterranean Sea was remarkably different from the SPE-DOM in the Atlantic Ocean inflow. Considering the shallow overturning cell of the Mediterranean Sea, the evolution of the molecular composition of SPE-DOM from the Levantine basin to the Strait of Gibraltar evidences the transformation of these materials since LIW is formed. As a result, a westward decrease of DOC concentrations and a lower proportion of unsaturated aliphatic compounds are observed, as well as an increase in average molecular weight and enrichment in unsaturation, oxygenation, state of degradation, and highly unsaturated compounds as the SPE-DOM is degraded. We found that the water mass origin and the formation time lead to distinct DOM molecular properties. Thus, pre-EMT deep waters formed in the Adriatic Sea presented less degraded DOM than deep waters formed in the Aegean Sea during the EMT. In addition, different varieties of deep

waters formed in the Adriatic Sea (pre- and post-EMT) presented different DOM molecular composition in spite of being formed in the same area. Consequently, the Mediterranean Sea constitutes a suitable model basin for future DOM studies as water bodies of different molecular composition can be observed in closest proximity. Taking advantages of forthcoming hydrographic cruises, it would be worthwhile to study the molecular composition of DOM in the Mediterranean waters at their formation sites and help to complete the picture of DOM molecular composition and turnover in the Mediterranean Sea.

References

- Amon, R. M., and R. Benner. 1996. Bacterial utilization of different size classes of dissolved organic matter. *Limnol. Oceanogr.* **41**: 41–51. doi:10.4319/lo.1996.41.1.0041
- Aristegui, J., C. M. Duarte, S. Agustí, M. Doval, X. A. Álvarez-Salgado, and D. A. Hansell. 2002. Oceanography: Dissolved organic carbon support of respiration in the dark ocean. *Science* **298**: 1967. doi:10.1126/science.1076746
- Benner, R., J. D. Pakulski, M. McCarthy, J. I. Hedges, and P. G. Hatcher. 1992. Bulk chemical characteristics of dissolved organic matter in the ocean. *Science* **255**: 1561–1564. doi:10.1126/science.255.5051.1561
- Benner, R., B. Biddanda, B. Black, and M. McCarthy. 1997. Abundance, size distribution, and stable carbon and nitrogen isotopic compositions of marine organic matter isolated by tangential-flow ultrafiltration. *Mar. Chem.* **57**: 243–263. doi:10.1016/S0304-4203(97)00013-3
- Bergamasco, A., and P. Malanotte-Rizzoli. 2010. The circulation of the Mediterranean Sea: A historical review of experimental investigations. *Adv. Oceanogr. Limnol.* **1**: 11–28. doi:10.1080/19475721.2010.491656
- Béthoux, J. P., P. Morin, C. Chaumery, O. Connan, B. Gentili, and D. Ruiz-Pino. 1998. Nutrients in the Mediterranean Sea, mass balance and statistical analysis of concentrations with respect to environmental change. *Mar. Chem.* **63**: 155–169. doi:10.1016/S0304-4203(98)00059-0
- Beuvier, J., and others. 2012. Spreading of the Western Mediterranean Deep Water after winter 2005: Time scales and deep cyclone transport. *J. Geophys. Res.* **117**: 1–26. doi:10.1029/2011JC007679
- Bray, J. R., and J. T. Curtis. 1957. An ordination of the upland forest communities of southern Wisconsin. *Ecol. Monogr. Ecol. Soc. Am.* **27**: 326–349. doi:10.2307/1942268
- Carlson, C. A. 2002. Chapter 4 – production and removal processes, p. 91–151. *In* D. A. Hansell and C. A. Carlson [eds.], *Biogeochemistry of marine dissolved organic matter*. Academic Press.
- Chen, H., A. Stubbins, E. M. Perdue, N. W. Green, J. R. Helms, K. Mopper, and P. G. Hatcher. 2014. Ultrahigh resolution mass spectrometric differentiation of dissolved organic matter isolated by coupled reverse osmosis–electrodialysis from

- various major oceanic water masses. *Mar. Chem.* **164**: 48–59. doi:10.1016/j.marchem.2014.06.002
- Chen, M., S. Kim, J. E. Park, H. J. Jung, and J. Hur. 2016. Structural and compositional changes of dissolved organic matter upon solid-phase extraction tracked by multiple analytical tools. *Anal. Bioanal. Chem.* **408**: 6249–6258. doi:10.1007/s00216-016-9728-0
- Cruzado, A. 1985. Chemistry of Mediterranean waters, p. 126–147. *In* R. Margalef [eds.], *The Western Mediterranean*. Pergamon Press.
- Dickson, R. R., and J. Brown. 1994. The production of North Atlantic Deep Water: Sources, rates, and pathways. *J. Geophys. Res.* **99**: 12319–12341. doi:10.1029/94JC00530
- Dittmar, T., B. Koch, N. Hertkorn, and G. Kattner. 2008. A simple and efficient method for the solid-phase extraction of dissolved organic matter (SPE–DOM) from seawater. *Limnol. Oceanogr.: Methods* **6**: 230–235. doi:10.4319/lom.2008.6.230
- Emelianov, M., J. Font, A. Turiel, C. Mullet, J. Solé, P. M. Poulain, A. Julià, and M. R. Vrià. 2006. Transformation of levantine intermediate water tracked by MEDARGO floats in the Western Mediterranean. *Ocean Sci.* **2**: 281–290. doi:10.5194/os-2-281-2006
- Flerus, R., O. J. Lechtenfeld, B. P. Koch, S. L. McCallister, P. Schmitt–Kopplin, R. Benner, K. Kaiser, and G. Kattner. 2012. A molecular perspective on the ageing of marine dissolved organic matter. *Biogeosciences* **9**: 1935–1955. doi:10.5194/bg-9-1935-2012
- Gascard, J. C. 1978. Mediterranean deep water formation baroclinic instability and oceanic eddies. *Oceanol. Acta* **1**: 315–330.
- Green, N. W., E. M. Perdue, G. R. Aiken, K. D. Butler, H. Chen, T. Dittmar, J. Niggemann, and A. Stubbins. 2014. An intercomparison of three methods for the large-scale isolation of oceanic dissolved organic matter. *Mar. Chem.* **161**: 14–19. doi:10.1016/j.marchem.2014.01.012
- Hansell, D. A. 2002. Chapter 15 – DOC in the global ocean carbon cycle, p. 685–715. *In* D. A. Hansell and C. A. Carlson [eds.], *Biogeochemistry of marine dissolved organic matter*. Academic Press.
- Hansell, D. A., C. A. Carlson, D. J. Repeta, and R. Schlitzer. 2009. Dissolved organic matter in the ocean a controversy stimulates new insights. *Oceanography* **22**: 202–211. doi:10.5670/oceanog.2009.109
- Hansman, R. L., T. Dittmar, and G. J. Herndl. 2015. Conservation of dissolved organic matter molecular composition during mixing of the deep water masses of the northeast Atlantic Ocean. *Mar. Chem.* **177**: 288–297. doi:10.1016/j.marchem.2015.06.001
- Hawkes, J. A., C. T. Hansen, T. Goldhammer, W. Bach, and T. Dittmar. 2016. Molecular alteration of marine dissolved organic matter under experimental hydrothermal conditions. *Geochim. Cosmochim. Acta* **175**: 68–85. doi:10.1016/j.gca.2015.11.025
- Hedges, J. I. 1992. Global biogeochemical cycles: Progress and problems. *Mar. Chem.* **39**: 67–93. doi:10.1016/0304-4203(92)90096-S
- Hertkorn, N., R. Benner, M. Frommberger, P. Schmitt–Kopplin, M. Witt, K. Kaiser, A. Kettrup, and J. I. Hedges. 2006. Characterization of a major refractory component of marine dissolved organic matter. *Geochim. Cosmochim. Acta* **70**: 2990–3010. doi:10.1016/j.gca.2006.03.021
- Hertkorn, N., M. Harir, B. P. Koch, B. Michalke, and P. Schmitt–Kopplin. 2013. High-field NMR spectroscopy and FTICR mass spectrometry: Powerful discovery tools for the molecular level characterization of marine dissolved organic matter. *Biogeosciences* **10**: 1583–1624. doi:10.5194/bg-10-1583-2013
- Holm-Hansen, O., C. J. Lorenzen, R. W. Holmes, and J. D. Strickland. 1965. Fluorometric determination of chlorophyll. *J. Cons. Int. Explor. Mer.* **30**: 3–15. doi:10.1093/icesjms/30.1.3
- Huertas, I. E., and others. 2012. Atlantic forcing of the Mediterranean oligotrophy. *Global Biogeochem. Cycles* **26**: GB2022. doi:10.1029/2011GB004167
- Jones, V., T. B. Meador, A. Gogou, C. Mignon, K. E. H. Penkman, M. J. Collins, and D. J. Repeta. 2013. Characterisation and dynamics of dissolved organic matter in the Northwestern Mediterranean Sea. *Prog. Oceanogr.* **119**: 78–89. doi:10.1016/j.pocean.2013.06.007
- Klein, B., and others. 2003. Accelerated oxygen consumption in eastern Mediterranean deep waters following the recent changes in thermohaline circulation. *J. Geophys. Res.* **108**: 8107. doi:10.1029/2002JC001454
- Koch, B. P., M. Witt, R. Engbrodt, T. Dittmar, and G. Kattner. 2005. Molecular formulae of marine and terrigenous dissolved organic matter detected by electrospray ionization Fourier transform ion cyclotron resonance mass spectrometry. *Geochim. Cosmochim. Acta* **69**: 3299–3308. doi:10.1016/j.gca.2005.02.027
- Koch, B. P., and T. Dittmar. 2006. From mass to structure: An aromaticity index for high-resolution mass data of natural organic matter. *Rapid Commun. Mass Spectrom.* **20**: 926–932. doi:10.1002/rcm.2386
- Koch, B. P., and T. Dittmar. 2016. Erratum: From mass to structure: An aromaticity index for high-resolution mass data of natural organic matter. *Rapid Commun. Mass Spectrom.* **30**: 250. doi:10.1002/rcm.7433 doi:10.1002/rcm.7433
- Koprivnjak, J. F., and others. 2009. Chemical and spectroscopic characterization of marine dissolved organic matter isolated using coupled reverse osmosis–electrodialysis. *Geochim. Cosmochim. Acta* **73**: 4215–4231. doi:10.1016/j.gca.2009.04.010
- Kujawinski, E. B. 2002. Electrospray ionization Fourier transform ion cyclotron resonance mass spectrometry (ESI FT–ICR MS): Characterization of complex environmental mixtures. *Environ. Forensics* **3**: 207–216. doi:10.1080/713848382
- Langdon, C. 2010. Determination of dissolved oxygen in seawater by Winkler titration using the amperometric

- technique, report N°. 14. In B. M. Sloyan and C. Sabine [eds.], GO-SHIP repeat hydrography manual: A collection of expert reports and guidelines. IOC/IOCCP.
- Laruelle, G. G., and others. 2009. Anthropogenic perturbations of the silicon cycle at the global scale: Key role of the land–ocean transition. *Global Biogeochem. Cycles* **23**: GB4031. doi:10.1029/2008GB003267
- Lascaratos, A., W. Roether, K. Nittis, and B. Klein. 1999. Recent changes in deep water formation and spreading in the eastern Mediterranean Sea: A review. *Prog. Oceanogr.* **44**: 5–36. doi:10.1016/S0079-6611(99)00019-1
- Lechtenfeld, O. J., G. Kattner, R. Flerus, S. L. McCallister, P. Schmitt-Kopplin, and B. P. Koch. 2014. Molecular transformation and degradation of refractory dissolved organic matter in the Atlantic and Southern Ocean. *Geochim. Cosmochim. Acta* **126**: 321–337. doi:10.1016/j.gca.2013.11.009
- López-Jurado, J.-L., C. González-Pola, and P. Vélez-Belchí. 2005. Observation of an abrupt disruption of the long-term warming trend at the Balearic Sea, western Mediterranean Sea, in summer 2005. *Geophys. Res. Lett.* **32**: L24606. doi:10.1029/2005GL024430
- Meador, T. B., and others. 2010. Biogeochemical relationships between ultrafiltered dissolved organic matter and picoplankton activity in the Eastern Mediterranean Sea. *Deep-Sea Res. Part II Top. Stud. Oceanogr.* **57**: 1460–1477. doi:10.1016/j.dsr2.2010.02.015
- Medeiros, P. M., M. Seidel, L. C. Powers, T. Dittmar, D. A. Hansell, and W. L. Miller. 2015. Dissolved organic matter composition and photochemical transformations in the northern North Pacific Ocean. *Geophys. Res. Lett.* **42**: 863–870. doi:10.1002/2014GL062663
- Millot, C. 1999. Circulation in the Western Mediterranean Sea. *J. Mar. Syst.* **20**: 423–442. doi:10.1016/S0924-7963(98)00078-5
- Mopper, K. D., J. Kieber, and A. Stubbins. 2015. Chapter 8–Marine photochemistry of organic matter: Processes and impacts, p. 389–450. In D. A. Hansell and C. A. Carlson [eds.], *Biogeochemistry of marine dissolved organic matter*. Elsevier.
- Oksanen, J., and others. 2016. vegan: Community ecology package. R package version 2.3–5. Available from <https://cran.r-project.org/web/packages/vegan/index.html>. Accessed May 22, 2017.
- Osterholz, H., T. Dittmar, and J. Niggemann. 2014. Molecular evidence for rapid dissolved organic matter turnover in Arctic fjords. *Mar. Chem.* **160**: 1–10. doi:10.1016/j.marchem.2014.01.002
- Osterholz, H., J. Niggemann, H. Giebel, M. Simon, and T. Dittmar. 2015. Inefficient microbial production of refractory dissolved organic matter in the ocean. *Nat. Commun.* **6**: 7422. doi:10.1038/ncomms8422
- Pinardi, N., and E. Masetti. 2000. Variability of the large scale general circulation of the Mediterranean Sea from observations and modelling: A review. *Palaeogeogr. Palaeoclimatol. Palaeoecol.* **158**: 153–174. doi:10.1016/S0031-0182(00)00048-1
- Pujo-Pay, M., and others. 2011. Integrated survey of elemental stoichiometry (C, N, P) from the western to eastern Mediterranean Sea. *Biogeosciences* **8**: 883–899. doi:10.5194/bg-8-883-2011
- Raeke, J., O. J. Lechtenfeld, M. Wagner, P. Herzsprung, and T. Reemtsma. 2016. Selectivity of solid phase extraction of freshwater dissolved organic matter and its effect on ultra-high resolution mass spectra. *Environ. Sci. Process. Impacts.* **18**: 918–927. doi:10.1039/c6em00200e
- Roether, W., B. B. Manca, B. Klein, D. Bregant, D. Georgopoulos, V. Beitzel, V. Kovacevic, and A. Luchetta. 1996. Recent changes in eastern Mediterranean deep waters. *Science* **271**: 333–335. doi:10.1126/science.271.5247.333
- Roether, W., B. Klein, V. Beitzel, and B. B. Manca. 1998. Property distributions and transient–tracer ages in Levantine Intermediate Water in the Eastern Mediterranean. *J. Mar. Syst.* **18**: 71–87. doi:10.1016/S0924-7963(98)00006-2
- Rossel, P. E., A. V. Vähätalo, M. Witt, and T. Dittmar. 2013. Molecular composition of dissolved organic matter from a wetland plant (*Juncus effusus*) after photochemical and microbial decomposition (1.25 yr): Common features with deep sea dissolved organic matter. *Org. Geochem.* **60**: 62–71. doi:10.1016/j.orggeochem.2013.04.013
- Santinelli, C. 2015. Chapter 13 – DOC in the Mediterranean Sea, p. 579–608. In D. A. Hansell and C. A. Carlson [eds.], *Biogeochemistry of marine dissolved organic matter*. Elsevier.
- Santinelli, C., L. Nannicini, and A. Seritti. 2010. DOC dynamics in the meso and bathypelagic layers of the Mediterranean Sea. *Deep-Sea Res. Part II Top. Stud. Oceanogr.* **57**: 1446–1459. doi:10.1016/j.dsr2.2010.02.014
- Santinelli, C., R. Sempéré, F. Van Wambeke, B. Charriere, and A. Seritti. 2012. Organic carbon dynamics in the Mediterranean Sea: An integrated study. *Global Biogeochem. Cycles* **26**: GB4004. doi:10.1029/2011GB004151
- Santinelli, C., C. Follett, S. Retelletti Brogi, L. Xu, and D. Repeta. 2015. Carbon isotope measurements reveal unexpected cycling of dissolved organic matter in the deep Mediterranean Sea. *Mar. Chem.* **177**: 267–277. doi:10.1016/j.marchem.2015.06.018
- Schlitzer, R. 2016. Ocean data view. <http://odv.awi.de>. Accessed May 22, 2017.
- Schneider, A., T. Tanhua, W. Roether, and R. Steinfeldt. 2014. Changes in ventilation of the Mediterranean Sea during the past 25 year. *Ocean Sci.* **10**: 1–16. doi:10.5194/os-10-1-2014
- Schroeder, K., J. Chiggiato, H. L. Bryden, M. Borghini, and S. B. Ismail. 2016. Abrupt climate shift in the Western Mediterranean Sea. *Sci. Rep.* **6**: 23009. doi:10.1038/srep23009
- Seidel, M., and others. 2014. Biogeochemistry of dissolved organic matter in an anoxic intertidal creek bank. *Geochim. Cosmochim. Acta* **140**: 418–434. doi:10.1016/j.gca.2014.05.038
- Seidel, M., and others. 2015. Molecular-level changes of dissolved organic matter along the Amazon River–to–ocean

- continuum. *Mar. Chem.* **177**: 218–231. doi:10.1016/j.marchem.2015.06.019
- Sokal, F. F., and F. J. Rohlf. 1995. *Biometry: The principles and practice of statistics in biological research*, 3rd ed. W. H. Freeman and Company.
- Stubbins, A., and others. 2010. Illuminated darkness: Molecular signatures of Congo River dissolved organic matter and its photochemical alteration as revealed by ultrahigh precision mass spectrometry. *Limnol. Oceanogr.* **55**: 1467–1477. doi:10.4319/lo.2010.55.4.1467
- Stubbins, A., and T. Dittmar. 2015. Illuminating the deep: Molecular signatures of photochemical alteration of dissolved organic matter from North Atlantic Deep Water. *Mar. Chem.* **177**: 318–324. doi:10.1016/j.marchem.2015.06.020
- Stuiver, M., P. D. Quay, and H. G. Ostlund. 1983. Abyssal water carbon-14 distribution and the age of the world oceans. *Science* **219**: 849–851. doi:10.1126/science.219.4586.849
- Tsimplis, M. N., and others. 2006. Chapter 4— changes in the oceanography of the Mediterranean Sea and their link to climate variability, p. 227–282. *In* P. Lionello, P. Malanotte-Rizzoli, and R. Boscolo [eds.], *Mediterranean climate variability*. Elsevier.
- UNESCO. 1985. The International System of Units (SI) in oceanography. UNESCO Tech. Paper. *Mar. Sci.* **45**: 1–124.
- UNESCO. 1986. Progress on oceanographic tables and standards 1983–1986. Work and recommendations of UNESCO/SCOR/ICES/IAPSO joint panel. UNESCO Tech. Pap. *Mar. Sci.* **50**: 1–59.
- UNESCO. 2010. The international thermodynamic equation of seawater: Calculation and use of thermodynamic properties. Intergovernmental Oceanographic Commission, Manuals and Guides No.56, UNESCO/IOC/SCOR/IAPSO (English), p. 196.
- Wu, P., K. Haines, and N. Pinardi. 2000. Toward an understanding of deep-water renewal in the Eastern Mediterranean. *J. Phys. Oceanogr.* **30**: 443–458. doi:10.1175/1520-0485(2000)030<0443:TAUODW>2.0.CO;2

Acknowledgments

The authors are grateful to the Captain, crew, technicians, and scientists aboard the R/V *Sarmiento de Gamboa* for their support during the cruise. We especially thank M. J. Pazó, V. Vieitez, M. Friebe, and I. Ulber for DOC measurements; K. Klapproth for support with FT-ICR-MS analysis; M. Manecki and B. E. Noriega for their help with data processing; and J. Niggemann for valuable discussions. This work was financed by the project HOTMIX (grant CTM2011-30010-C02-01-MAR and 02-MAR) and the project FERMIO (MINECO, CTM2014-57334-JIN), both co-financed with FEDER funds. A.M.M.-P. was funded by a predoctoral fellowship (reference BES-2012-056175) and a short stay fellowship (reference EEBB-I-14-08926) from the Spanish Ministry of Economy and Competitiveness. M. N.-C. was partially supported by the CSIC Program “Junta para la Ampliación de Estudios,” co-financed by the ESF (reference JAE DOC 040), co-financed with FEDER funds.

Conflict of Interest

None declared.

Submitted 14 June 2016

Revised 16 February 2017; 27 April 2017

Accepted 05 May 2017

Associate editor: Peter Hernes